

# Optical transitions in the isoelectronically doped semiconductor GaP:N: An evolution from isolated centers, pairs, and clusters to an impurity band

Yong Zhang,\* B. Fluegel, and A. Mascarenhas  
National Renewable Energy Laboratory, Golden, Colorado 80401

H. P. Xin and C. W. Tu  
Department of Electrical and Computer Engineering, University of California, San Diego, La Jolla, California 92093  
(Received 7 February 2000; revised manuscript received 6 April 2000)

In heavily nitrogen doped GaP, we show how isoelectronic doping results in an impurity band, and how this is manifested as a large band-gap reduction and an enhanced band-edge absorption. Heavily doped GaP:N or  $\text{GaP}_{1-x}\text{N}_x$  exhibits properties characteristic of both direct and indirect gap semiconductors. Exciton bound states associated with perturbed nitrogen pair centers and larger GaN clusters are observed. This paper indicates that to properly describe the properties of an impurity band, a hierarchy of impurity complexes needs to be considered. Our data also suggest that the excitonic effect plays a role in the impurity band formation and band-gap reduction.

## I. INTRODUCTION

The electronic and optical properties of heavily doped semiconductors have been very extensively studied. However, the focus has mainly been on the nonisovalent impurities that usually behave as donors or acceptors.<sup>1,2</sup> Donors or acceptors generate a series of hydrogenlike bound states in the host semiconductor. Thus, heavy doping results in the formation of an impurity band located below the intrinsic band gap of the host, which effectively reduces the band gap and brings about many other interesting phenomena, such as, the so-called Mott transition. On the other hand, a host semiconductor with isoelectronic impurities is typically viewed as an alloy.<sup>3</sup> In the dilute limit, the effect of isoelectronic impurities is negligible,<sup>4</sup> as long as the impurity does not introduce a bound state. There are, however, a few interesting cases in which isoelectronic impurities do generate bound states. These bound states can be either donorlike (e.g., GaP:Bi and CdS:Te) or acceptorlike (e.g., GaP:N and CdS:O).<sup>5</sup> The properties of these isoelectronic doped systems have been well studied in the impurity limit, and there are several reviews on this subject.<sup>6-11</sup> Although in the early study on isoelectronic impurities, precautions for avoiding the impurity band effect were pointed out,<sup>12</sup> experimentally, the actual doping levels rarely reached the threshold for the formation of an impurity band until recently, when the newer growth techniques such as molecular-beam epitaxy and metal-organic chemical vapor deposition were used. Nevertheless, a heavy doping induced redshift of the fluorescence was reported by Aten *et al.* in the CdS:Te system for impurity concentrations higher than  $10^{-4}$  mole fractions,<sup>13</sup> presumably due to the impurity band effect.

Owing to various potential device applications, in the past few years, heavily doped GaAs:N, GaInAs:N, InP:N, and GaP:N have attracted a great deal of attention. The physical properties of these systems have frequently been described by viewing them in the framework of alloys.<sup>14-25</sup> Thus, the N-induced large band-gap reduction and giant bowing observed in these systems have led to the perception that they are abnormal alloys. However, we have recently pointed out that these systems are more appropriately viewed as heavily

doped semiconductors rather than as alloys.<sup>11,26,27</sup> Within the framework of heavily doped semiconductors, the abnormalities can be viewed as trivial consequences of impurity band formation, as in the cases of nonisovalent doping. In fact, these semiconductors serve as ideal systems for investigating impurity band effects without the complications encountered in charged doping systems.<sup>1,2</sup> For instance, we were able to experimentally obtain the variation of the electron effective mass as a function of doping level resulting from the impurity band effect in heavily doped GaAs:N.<sup>27</sup> For charged doping systems, such an effect has only been discussed theoretically.<sup>1,2</sup>

GaP:N is perhaps the most well-studied isoelectronic impurity system in the impurity limit.<sup>6-11</sup> Compared to GaAs:N, that is the most intensively studied system for the past few years, GaP:N has not only a large doping range for the impurity limit ( $\sim 10^{15}$ – $20^{20}$  cm<sup>-3</sup>) but also a relatively high-critical concentration for the formation of the impurity band,<sup>27</sup> which makes it a unique system for investigating the impurity band effects that results from heavy isoelectronic doping. At a very low-doping level ( $[\text{N}] < 10^{17}$  cm<sup>-3</sup>), only one emission line (A line) from the exciton bound to isolated N center is observed, together with its phonon sidebands; at a higher doping level (up to  $[\text{N}] \sim 10^{19}$  cm<sup>-3</sup>), a series of emission lines (NN<sub>i</sub> lines) from different N-N pairs, appear in an energy range  $\sim 140$  meV below the band gap, together with their phonon sidebands.<sup>28</sup> Recently, the deepest N-N pair bound state, NN<sub>1</sub>, was shown to be observable up to concentrations of  $[\text{N}] \sim 1 \times 10^{20}$  cm<sup>-3</sup> or  $x = 0.4\%$ .<sup>15,29-31</sup> At a higher N concentration, the spectrum was significantly broadened and no structures were identified. The authors of Refs. 15 and 29 concluded that for  $x > 0.4\%$ ,  $\text{GaP}_{1-x}\text{N}_x$  remained an indirect gap semiconductor alloy, based on the fact that the luminescence efficiency decreased with increasing N doping and the absorption edge exhibited the characteristic energy dependence of an indirect gap semiconductor (i.e., the square dependence). The band-gap reduction and bowing were explained by a dielectric theory of electronegativity.<sup>32</sup> Later, the authors of Refs. 30 and 31 pointed out that the for  $x > 0.4\%$ , N-doped GaP could be viewed as a  $\text{GaP}_{1-x}\text{N}_x$  alloy, and that the origin of the band-

gap reduction was the impurity band effect arising from the isolated N center. This idea was further examined by using a tight-binding model calculation,<sup>33</sup> which concluded that the newly formed conduction band had indirect gap character. Very recently, with improved sample quality, we observed<sup>34</sup> that for N-doped GaP samples with a doping level  $x$  between 1% and 3%, the room temperature absorption edge appeared to have the characteristic energy dependence of a direct gap semiconductor (i.e., the square-root dependence), and that these samples luminesced strongly even at room temperature. Also, a pseudopotential supercell calculation<sup>35</sup> indicated that the band structure of the  $\text{GaP}_{1-x}\text{N}_x$  alloy changed from indirect to direct at a critical composition of  $x_c = 3\%$ , and that the interband transition matrix element continued to increase until  $x \sim 10\%$ . Since the lowest N-N pair state is  $\text{NN}_1$  and not the isolated center A, our paper reveals that the evolution of the  $\text{NN}_1$  center and the possibility of forming larger N clusters with increased doping level have been overlooked in all the previous modeling.

In this paper, we follow the process of evolution of various N-related optical transitions, including those associated with newly observed N bound states, in a set of samples with  $x$  varying from  $1.24 \times 10^{19}$  to  $7.66 \times 10^{20} \text{ cm}^{-3}$  or from  $x = 0.05\%$  to 3.1%. Our results show that a hierarchy of N complexes including isolated N, N-N pairs, N-N-N triplets, etc., that generate different bound states, has to be included in order to describe properly the electronic structure of heavily doped GaP:N.

## II. SAMPLES AND EXPERIMENTS

The  $\text{GaP}_{1-x}\text{N}_x$  samples were grown on (100) GaP substrates with 2000 Å thick buffer layers by gas-source molecular beam epitaxy in a modified Varian Gen-II system. 7N elemental Ga and thermally cracked  $\text{PH}_3$  at 980 °C were used. High-purity  $\text{N}_2$  was injected through a N radical beam source (Oxford Applied Research Model MPD21) operated at a radio frequency of 13.56 MHz to generate active N species. For the GaP buffer layers, the growth temperature was 640 °C. For  $\text{GaP}_{1-x}\text{N}_x$  layers, the growth temperature was decreased to 520 °C to incorporate N. The N composition was determined by high-resolution x-ray rocking curve (XRC) measurement and dynamical theoretical simulations. The epilayer thickness are 2500 Å for six samples with  $x = 0.05\%$ , 0.12%, 0.24%, 0.43%, 0.60%, 0.81%, and 7500 Å for another seven samples with  $x = 0\%$  (nominal), 0.70%, 0.90%, 1.3%, 2.0%, 2.3%, and 3.1%, respectively. In (400) XRC measurements, the Pendelloesung fringes were well resolved for these 2500 Å thick epilayers, indicating high-crystalline quality. For the 7500 Å epilayers with relatively high  $x$  values ( $x \geq 1.3\%$ ), the epilayers were found to be partially relaxed. Photoluminescence (PL) was measured with samples in a closed cycle cryostat at  $\sim 10$  K. The detection system included a SPEX1403 double-grating spectrometer and a cooled RCA C31034 GaAs photomultiplier tube. The excitation source was a 532-nm laser. The typical power used was 100  $\mu\text{W}$ , corresponding to an excitation density of  $\sim 1 \text{ W/cm}^2$ . A dye laser using the R6G dye was used for selective excitation PL measurements. A monochromator was used for eliminating possible dye fluorescence. Transmission (absorption) measurements were per-

formed at 4 K, using a liquid Helium Dewar and a Spex 270M spectrometer with a charge coupled detector.

## III. RESULTS AND DISCUSSIONS

Figure 1 shows the PL spectra for samples with  $x \leq 0.9\%$ . Up to the highest  $x$  value, PL spectra for all samples in this group contain some identifiable fine structure. As shown in Fig. 1(a), these spectra reproduce a well-known trend which is that the dominant emission shifts to lower energy with increasing  $x$ , due to the exciton transfer effect.<sup>36</sup> The insert of Fig. 1(a) is a PL spectrum for the nominally undoped sample that actually has a residual doping level estimated to be  $\sim 10^{17} \text{ cm}^{-3}$ . The A line as well as several  $\text{NN}_i$  transitions can be observed simultaneously. With the doping level  $x$  changed more continuously over an extended range, we can now follow the evolution of all the N-related transitions much more closely than previously.<sup>15,29-31</sup> First, as shown in Fig. 1(b), starting from the shallower  $\text{NN}_i$  centers, the PL linewidth gradually broadens and shifts to lower energy, which suggests that an intercenter interaction is taking place with increasing  $x$ , and that this interaction is easier to occur for less localized or shallower centers. Second, the emission intensity of the phonon sideband region is enhanced relative to the corresponding zero-phonon line, as shown in Fig. 1(b) for  $\text{NN}_3$  and Fig. 1(c) for  $\text{NN}_1$ . Such an observation has been reported before, and was explained as the consequence of wave function delocalization, i.e., an enhancement of the phonon side band and a decrease in the zero-phonon line.<sup>37</sup> Interestingly, our selective excitation PL with excitation energy below the  $\text{NN}_1$  zero-phonon line reveals that there exist real bound states in the phonon sideband region of the  $\text{NN}_1$  center. The results are shown in Fig. 2, and will be discussed later. Thus, the observed enhancement is explained as the result of an increase in the density of these bound states with increasing doping level  $x$ . Some of these bound states are likely to be pair centers under the perturbation of relatively remote nitrogen centers, which have a similar origin as the so-called V band below the A line [which is shown in the insert of Fig. 1(a)].<sup>38</sup> The bound states found inside the V band have been shown to be perturbed isolated N centers.<sup>39</sup> Another reason for the quenching of the  $\text{NN}_1$  zero-phonon line is the self-absorption effect<sup>28</sup> due to the increasing  $\text{NN}_1$  concentration. Note that the N-local mode sideband remains visible up to a doping level  $x = 0.9\%$  with only a small energy shift, which indicates that the  $\text{NN}_1$  state retains most of its characters as an impurity center even at such a high-doping level. The quenching of those higher energy phonon sidebands of  $\text{NN}_1$  can also be explained as the result of absorption effect of the bound states below  $\text{NN}_1$ . Thirdly, for  $x \geq 0.43\%$ , a new peak appears at 2.071 eV that does not match the energy of any known phonon sideband of  $\text{NN}_1$ .<sup>40</sup> We tentatively attribute this peak to the zero-phonon line of a N cluster (NC), most likely a triplet, with its LO phonon sideband at 2.023 eV and local mode (Loc) sideband at 2.009 eV. This assignment will be further corroborated by the selective excitation measurements, which will be discussed below.

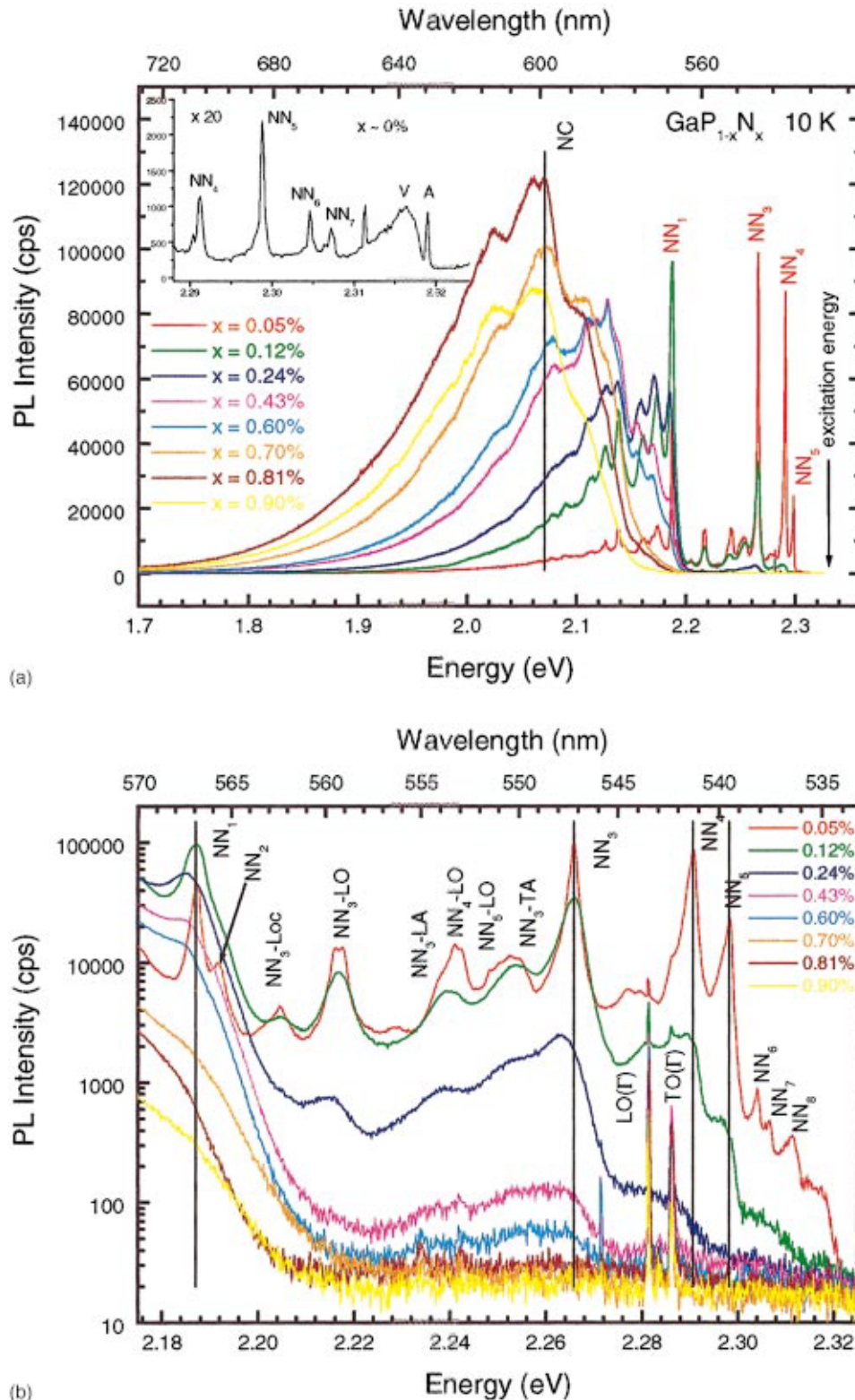
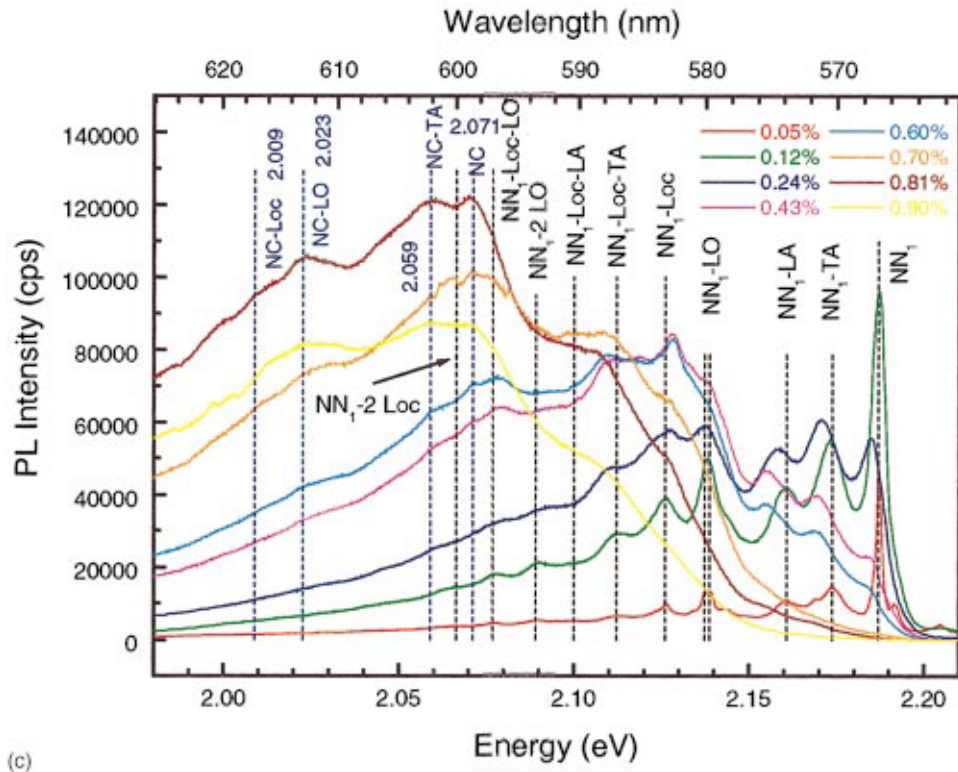


FIG. 1. (Color) PL spectra for GaP:N with low to intermediate nitrogen doping levels under above band-gap excitation. (a) Full spectral range, (b) zoom-in to the higher-energy portion, and (c) zoom-in to the lower-energy portion.

To further examine the origin of the transitions below the  $NN_1$  line, we perform selective excitation measurement with excitation energy well below that of the  $NN_1$  zero-phonon line. Figures 2(a)–2(c) show PL spectra of four samples with  $x=0.05\%$ ,  $0.43\%$ ,  $0.60\%$ , and  $0.81\%$  under two excitation energies (2.1354 eV and 2.1014 eV). Results for other exci-

tation energies (not shown) are qualitatively similar to that shown in Fig. 2. For the  $x=0.05\%$  sample, included in Fig. 2(a), there is almost no emission except for Raman peaks. However, for higher  $x$  samples, as shown in Fig. 2(a)–Fig. 2(c), beside the Raman peaks, we observe two transitions, labeled as  $NN'_1$  and NC, together with their phonon side-



(c)

FIG. 1. (Continued.)

bands. The transition energy of  $NN'_1$  shift on varying the excitation energy, with its zero-phonon peak a few meV below the excitation energy and a set of phonon sidebands similar to those of  $NN'_1$  centers. The energy of NC transition remains nearly stationary at around 2.07 eV on varying the excitation energy, but shifts slightly with increasing doping level  $x$  (the shift is visible between  $x=0.60\%$  and  $0.81\%$ ). This second transition is in fact the one seen under the above band-gap excitation, as shown in Fig. 1(c), and is attributed to a N cluster with more than two N atoms. Also, we find that the shift between the excitation energy and that of  $NN'_1$ ,  $\delta E$ , is proportional to the doping level  $x$ . Such a shift is similar to the Stokes shift between the emission and absorption band observed for the A line in the dilute  $\text{GaP}_{1-x}\text{As}_x:\text{N}$  system, where the shift was explained in terms of the inhomogeneous broadening of the A line due to the statistical distribution of the (P,As) configurations (i.e., a group V sublattice site can be either occupied by a P atom or a As atom) near a single N center,<sup>41</sup> and the very efficient exciton transfer within the broadened band.<sup>42</sup> Here, it is the distribution of the (P,N) configuration away from a  $NN_1$  center that causes the broadening effect, and gives rise to the  $NN'_1$  transition. On the other hand, a sufficiently nearby fluctuation of the (P,N) configuration is expected to form a new discrete bound state like NC with a well-defined binding energy that is larger than that of  $NN_1$ . In general, we expect that the further away the states are from  $NN_1$ , the stronger they are perturbed, which is supported by the  $x$  dependence of the PL intensity with different excitation energies. We find that from  $x=0.43\%$  to  $0.81\%$ , the  $NN'_1$  intensity changes by a factor of 3.0, 5.8, and 7.8 when excited at 2.1354, 2.1111, and 2.1014 eV, respectively. Under low-excitation density, the PL intensity is expected to be proportional to the density-of-states

(DOS) at the excitation energy. Since the  $\text{DOS} \propto [N]^2$  for pair states and the  $\text{DOS} \propto [N]^3$  for triplet states, we notice that the observed ratios are close to  $(0.81/0.43)^2 = 3.5$  for the highest-excitation energy and  $(0.81/0.43)^3 = 6.7$  for the lowest-excitation energy, which indicates that there are more triplelike states in the lower portion and more pairlike states in the upper portion of the broadband. Of course, the exact intensity dependence on  $x$  depends on many other parameters and processes, e.g., the transition rate and various energy-transfer processes.<sup>43</sup> In Ref. 43, possible triples centers ( $NN_\alpha N_\beta$  with  $\alpha < 10$  and  $\beta > 10$ ) were included in modeling the PL intensity of the  $NN_i$  centers; and in Ref. 44, a strong asymmetric broadening on the low-energy side of the  $NN_3$ ,  $NN_4$ , and  $NN_5$  bands was attributed to  $NN_\alpha N_\beta$  with  $\alpha < 10$  and  $\beta > 10$ . However, there had not been any experimental observation of discrete triplet states like NC, except for the possibility that  $NN_2$  might be a triplet rather than a pair.<sup>45</sup> Also, it is worth mentioning that a new Raman peak (denoted by\*) appears between the LO( $\Gamma$ ) and TO( $\Gamma$ ) modes with an energy of  $47.7 \pm 0.1$  meV when  $x \geq 0.43\%$ .

Figure 3 shows the energy shift  $\delta E$ , as a function of excitation energy for three samples with  $x=0.43\%$ ,  $0.60\%$ , and  $0.81\%$ .  $\delta E$  remains nearly a constant for each sample (they are 4.6–4.9, 5.2–5.5, and 7.5–7.7 meV, respectively). Beside the mechanism of exciton transfer we have proposed above, there are in fact two other mechanisms that are likely to be the origin for the energy shift. One is the electron-hole exchange splitting between the  $J=1$  and  $J=2$  components of the bound exciton state.<sup>28</sup> This mechanism was used for explaining the similar shift observed either in the V band of GaP:N in Ref. 39 or in the  $N_x$  band of  $\text{GaAs}_{1-y}\text{P}_y:\text{N}$  in Ref. 46. However, considering the fact that (i) the exchange splitting remains nearly a constant of 0.8 meV, whereas the ex-

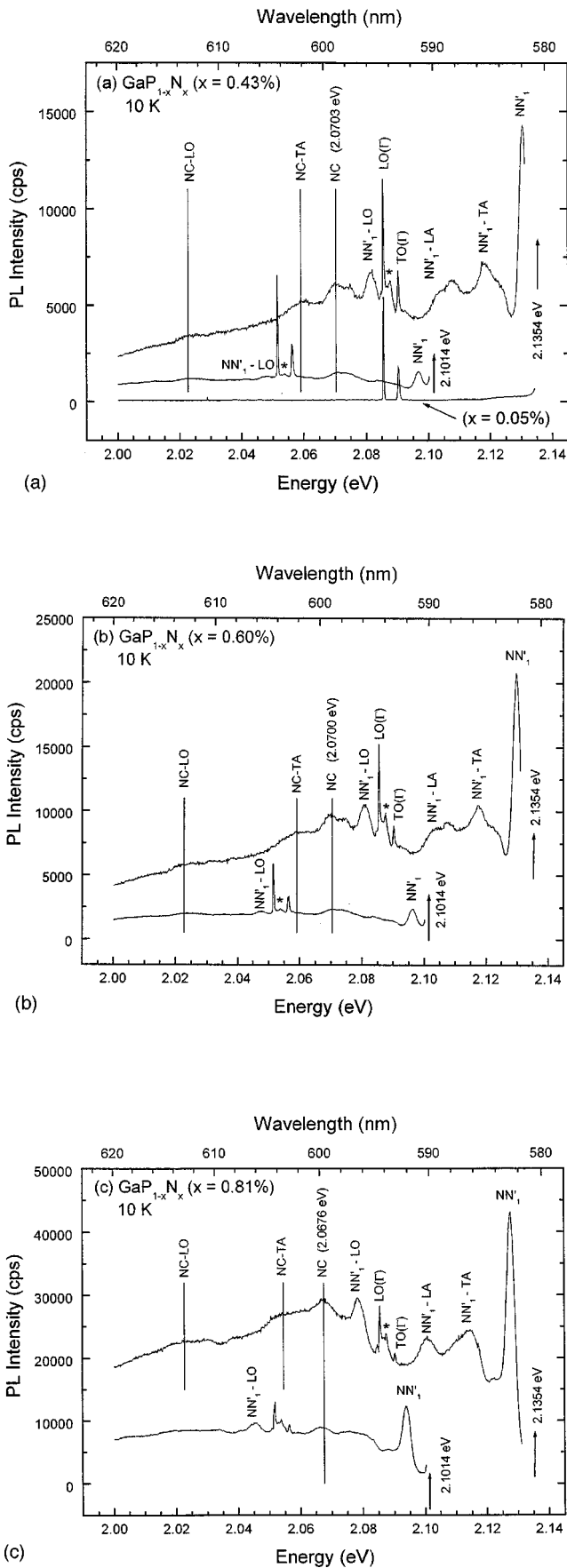


FIG. 2. PL spectra for GaP:N with intermediate nitrogen concentration under selective excitations. “\*” indicates a new Raman line.

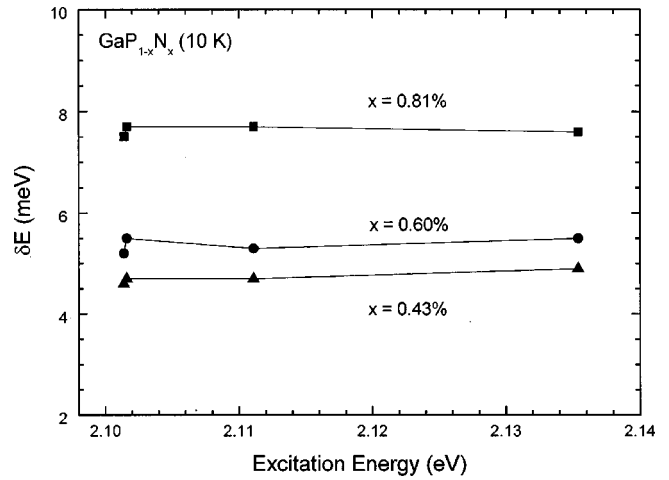


FIG. 3. The energy shift  $\delta E$  as a function of the excitation energy and composition.

citon binding energy varies more than 130 meV from the A line to NN<sub>1</sub>, (ii)  $\delta E$  does not change with varying excitation energy for a fixed N composition  $x$ , but (iii) changes with varying  $x$  for a fixed excitation energy or binding energy, we may exclude the exchange splitting as the origin of the observed shift. The other possible mechanism is the epitaxial strain experienced by the GaP<sub>1-x</sub>N<sub>x</sub> layer on GaP. Such a strain effect has recently been observed in GaAs<sub>1-x</sub>N<sub>x</sub> as a valence-band splitting.<sup>26</sup> Using the deformation potential  $b = -1.5$  eV for GaP,<sup>47</sup> we obtain valence-band splittings of 4.5, 6.3, and 8.6 meV for  $x=0.43\%$ ,  $0.60\%$  and  $0.81\%$ , respectively. These numbers are indeed quite close to the energy shifts we have observed. However, to associate the energy shift with the strain splitting, one has to assume that the bound exciton created at the higher-energy state with its energy level matching the excitation energy relaxes to the lower-energy state and recombines locally. Since very efficient spatial energy transfer (with respect to the relatively long radiative decay time) always occurs in GaP:N and GaAs<sub>y</sub>P<sub>1-y</sub>:N,<sup>36,42</sup> the transfer effect is likely to dominate the decay dynamics. Although further investigation is needed for understanding the detailed recombination mechanism for the NN<sub>1</sub>' transition, there is little doubt about the fact that NN<sub>1</sub>' is associated with perturbed NN<sub>1</sub> centers.

Figure 4 shows PL spectra for samples with doping level  $x \geq 0.9\%$ . For samples with  $x \geq 1.3\%$ , PL spectra do not show any well-defined features, and their peak positions shift to lower energies with increasing  $x$ . The PL intensity decreases for  $x \geq 0.9\%$ , which is probably due to decreased sample quality.<sup>34</sup> For the  $x = 3.1\%$  sample, the peak position appears at  $\sim 1.85$  eV where the absorption is already very weak (see Fig. 4), and the PL extends to an energy as low as 1.4 eV. Such a long emission tail has also been observed in heavily doped GaAs:N. The origin of the long emission tail is unclear at this time, and will be the subject of a future study.

Figure 5 shows absorption spectra for three samples with  $x = 0.9\%$ ,  $1.3\%$ , and  $3.1\%$ , respectively. For the  $x = 0.9\%$  sample, three absorption peaks are resolved below the GaP free exciton band gap of 2.328 eV.<sup>28</sup> Their energies shift slightly with increasing  $x$ , but remain close to those of NN<sub>1</sub>, NN<sub>3</sub>, and the A line, respectively. On further increasing  $x$ ,

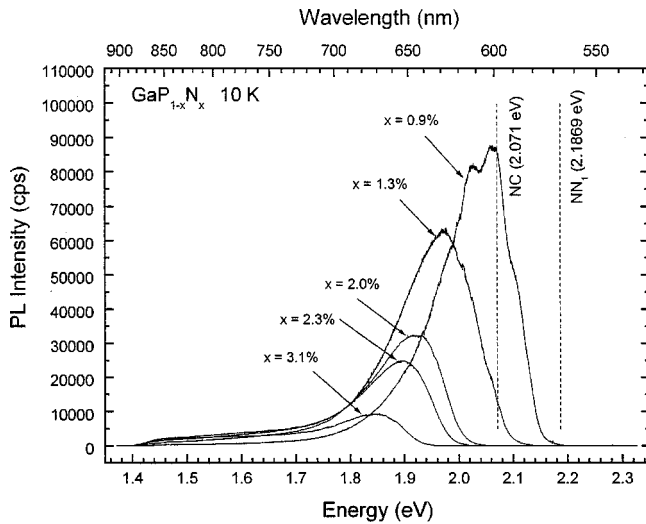


FIG. 4. PL spectra for GaP:N with high-nitrogen concentration under above band-gap excitation.

these absorption peaks are further broadened. Even for the  $x=3.1\%$  sample, the trace of the  $NN_1$  feature still persists. These results indicate that the new conduction band is formed by the superposition of a hierarchy of nitrogen induced bound states that are all inhomogeneously broadened due to the impurity band effect. The absorption coefficients for the  $x=3.1\%$  sample are found to be  $1.7 \times 10^4$  and  $2.2 \times 10^4 \text{ cm}^{-1}$  at the energies of  $NN_1$  and the A line, respectively. Although the absorption profiles cannot be simply described by either direct or indirect transition theory, it seems that these relatively large values are supportive of the view that heavily doped GaP:N is a direct gap material.<sup>34</sup> However, the origin for the large absorption coefficient is in fact the same as that for the “quasidirect” transition<sup>8</sup> in the dilute limit where the localization of the impurity potential introduces a  $\Gamma$  component in the impurity wave function. The absorption coefficient for the A line is known to be  $\alpha_A = 3.8 \times 10^{-15} [N] \text{ cm}^{-1}$ .<sup>48</sup> For  $NN_1$ , the absorption coefficient

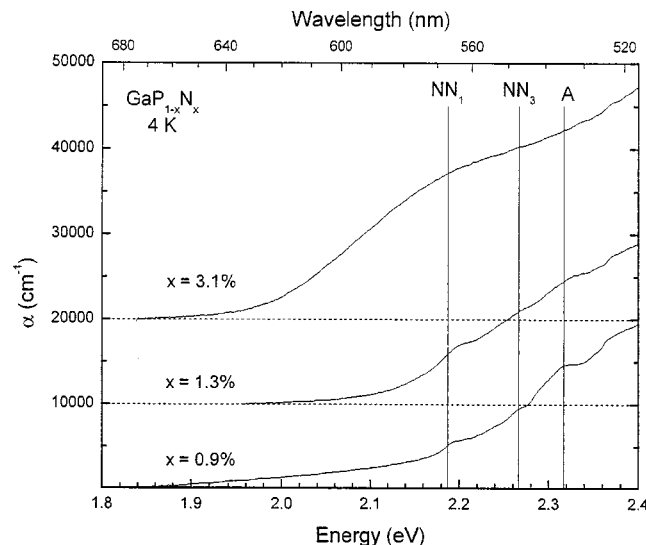


FIG. 5. Absorption spectra of GaP:N with high-nitrogen concentrations. The spectra of  $x=1.3\%$  and  $3.1\%$  samples are shifted vertically for clarity.

can be estimated using  $\alpha_{NN_1} \approx 3 \times 10^{-15} [NN_1] \text{ cm}^{-1}$ , where  $[NN_1]$  is the concentration of the  $NN_1$  centers.<sup>28,48</sup> If one applies these formulas to the sample with  $x=3.1\%$ , one obtains  $\alpha_A \approx 3 \times 10^6 \text{ cm}^{-1}$  and  $\alpha_{NN_1} \approx 10^5 \text{ cm}^{-1}$ . Noting the fact that all these bound states have very small linewidths ( $<1 \text{ meV}$ ) in the dilute limit, and that they get severely broadened (more for the A line than for the  $NN_1$ ) due to the impurity band effect, the experimentally observed values are quite reasonable. In spite of the large absorption coefficient, the impurity band still retains its indirect characteristic of having a relatively long lifetime. For the  $x=3.1\%$  sample, the PL decay time is found to be  $\sim 60$  and  $\sim 40 \text{ ns}$  for  $T=4$  and  $20 \text{ K}$ , respectively, which is qualitatively consistent with previously reported results for similar doping levels.<sup>49</sup> Here we have simply used the decay time at the  $1/e$  intensity point as a measure of the PL decay. In general, the decay process is nonexponential. The details for the decay dynamics will be reported elsewhere. We would like to point out that the obtained PL decay time in fact sets a lower limit for the radiative decay time that is apparently much longer than that for the free exciton in GaAs ( $\sim 3 \text{ ns}$ ).<sup>50</sup> Thus, because it shares the characteristics of both direct and indirect gap materials, GaP:N is perhaps a more attractive material for certain device applications (e.g., solar cells) than GaAs:N.

The simplest view of a heavily doped semiconductor is to assume that the impurities are uniformly distributed with a separation of  $[N]^{-1/3}$ . This simplification has in fact been adopted in many recent super-cell calculations for Group-III-V-N alloys.<sup>21,24,25,33,35</sup> However, in reality, the impurities are randomly distributed. Thus, the formation of pair or triplet centers is inevitable, with their concentration proportional to  $[N]^2$  and  $[N]^3$ , respectively. For instance, when  $x=1\%$ , we have  $[N] \approx 2.5 \times 10^{20} \text{ cm}^{-3}$ ,  $[NN_{[110]}] \approx 1.5 \times 10^{19} \text{ cm}^{-3}$ , and  $[NN_{[110]}N_{[200]}] \approx 5.9 \times 10^{17} \text{ cm}^{-3}$ . Since pair or triplet centers tend to have larger binding energies than an isolated center, they naturally play a key role in determining the properties of the new effective band edge in these Group-III-V-N alloys.

The results of Fig. 1 reveal that impurity band formation occurs sequentially for different  $NN_i$  centers on increasing the N doping level, i.e., following the order of their binding energies. A simple criterion for estimating the critical doping levels ( $x_0$ ) for impurity band formation is given by  $2r_0 = n^{-1/3}$ ,<sup>2</sup> where  $n$  is the concentration of the centers considered, and  $r$  is the “radius” of the impurity wave function (in our case, the wave function of the bound electron). According to the so-called HTL (Hopfield, Thomas, and Lynch) model,<sup>5</sup> the electron is very tightly bound to the isoelectronic impurity in GaP:N, which makes it rather difficult for inter-center coupling to occur. For a localized center, as a rough estimate, one can use  $r_0 = (2mE_b/\hbar^2)^{-1/2}$ , where  $E_b$  is the binding energy and  $m$  is the effective mass.<sup>51</sup> For  $NN_1$ , using  $E_b = 124 \text{ meV}$ ,<sup>52</sup> we have  $r_0 = 6.4 \text{ \AA}$ , which yields a critical doping level  $x_0 = 5.6\%$ . This critical value seems too high when compared to our experimental data. In fact, our PL data of Fig. 1 indicate that the linewidth broadening for  $NN_1$  has already occurred at least at a doping level of  $x=0.24\%$ , yet the  $NN_1$  transition remains quite well-defined even at  $x=1.3\%$  in the absorption data of Fig. 4. We would like to point out that there is another mechanism that will

assist inter-center coupling, i.e., the excitonic effect. The bound excitons associated with deep  $NN_1$  centers have been shown to be acceptorlike with a binding energy of  $\sim 40$  meV.<sup>52</sup> The radius for the bound hole state is estimated to be  $\sim 16$  Å.<sup>53</sup> Assuming  $r_0 = 16$  Å, we get  $x_0 = 1.4\%$ . This is a very reasonable value, judging from the experimental data. Although the exact value for  $x_0$  may not be so important, this analysis reveals the role of the bound hole in serving as a mediator for assisting intercenter exciton-exciton coupling, and that the hole binding energy constitutes part of the band-gap reduction in optical measurements.

#### IV. SUMMARY AND CONCLUSIONS

In summary, we have demonstrated in heavily doped GaP:N the formation of a nitrogen related impurity band that comprises the contributions from a hierarchy of nitrogen bound states. Optical transitions associated with excitons

bound to perturbed NN pair centers and a N cluster are observed. The mechanism for the enhanced band-edge absorption is explained in terms of an impurity band effect. Our data also suggest that intercenter exciton-exciton coupling assists the impurity band formation, and that the hole binding energy contributes to the band-gap reduction.

#### ACKNOWLEDGMENTS

The work at NREL was supported by the U.S. Department of Energy under Contract No. DE-AC36-83CH10093 and by the NREL DDRD under program No. 0659.0004, and the work at UCSD was partially supported by Midwest Research Institute under subcontractor No. AAD-9-18668-7 from NREL. We thank Kim Jones for help with sample preparation.

\*Email: yzhang@nrel.gov

- <sup>1</sup>B. I. Shklovskii and A. L. Efros, *Electronic Properties of Doped Semiconductors* (Springer-Verlag, Berlin, 1984).
- <sup>2</sup>E. F. Schubert, *Doping in III-V Semiconductors* (Cambridge University Press, Cambridge, 1993).
- <sup>3</sup>A. B. Chen and A. Sher, *Semiconductor Alloys* (Plenum, New York, 1995).
- <sup>4</sup>J. P. Laurenti, P. Roentgen, K. Wolter, K. Seibert, H. Kurz, and J. Camassel, *Phys. Rev. B* **37**, 4155 (1988).
- <sup>5</sup>J. J. Hopfield, D. G. Thomas, and R. T. Lynch, *Phys. Rev. Lett.* **17**, 312 (1966).
- <sup>6</sup>P. J. Dean, *J. Lumin.* **1-2**, 398 (1970).
- <sup>7</sup>W. Czaja, *Festkoerperprobleme* **11**, 65 (1971).
- <sup>8</sup>M. G. Craford and N. Holonyak, Jr., in *Optical Properties of Solids: New Developments*, edited by B. O. Seraphin (North-Holland, Amsterdam, 1976), pp. 187.
- <sup>9</sup>R. J. Nelson, Excitons in Semiconductor Alloys, in *Excitons*, edited by E. I. Rashba and M. D. Sturge (North-Holland, Amsterdam, 1982), p. 319.
- <sup>10</sup>V. K. Bazhenov and V. I. Fistul', *Fiz. Tekh. Poluprovodn.* **8**, 1345 (1984) [*Sov. Phys. Semicond.* **18**, 843 (1984)].
- <sup>11</sup>Yong Zhang and W.-K. Ge, *J. Lumin.* **85**, 247 (2000).
- <sup>12</sup>J. W. Allen, *J. Phys. C* **4**, 1936 (1971).
- <sup>13</sup>A. C. Aten, J. H. Haanstra, and H. de Vries, *Philips Res. Rep.* **20**, 395 (1965).
- <sup>14</sup>M. Weyers, M. Sato, and H. Ando, *Jpn. J. Appl. Phys., Part 2* **31**, L853 (1992).
- <sup>15</sup>J. N. Baillargeon, K. Y. Cheng, G. E. Hofler, P. J. Pearah, and K. C. Hsieh, *Appl. Phys. Lett.* **60**, 2540 (1992).
- <sup>16</sup>W. G. Bi and C. W. Tu, *J. Appl. Phys.* **80**, 1934 (1996).
- <sup>17</sup>W. Shan, W. Walukiewicz, J. W. Ager III, E. E. Haller, J. F. Geisz, D. J. Friedman, J. M. Olson, and S. R. Kurtz, *Phys. Rev. Lett.* **82**, 1221 (1999).
- <sup>18</sup>J. D. Perkins, A. Mascarenhas, Y. Zhang, J. F. Geisz, D. J. Friedman, J. M. Olson, and S. R. Kurtz, *Phys. Rev. Lett.* **82**, 3312 (1999).
- <sup>19</sup>A. Rubio and M. L. Cohen, *Phys. Rev. B* **51**, 4343 (1995).
- <sup>20</sup>J. Neugebauer and C. G. Van de Walle, *Phys. Rev. B* **51**, 10 568 (1995).
- <sup>21</sup>S.-H. Wei and A. Zunger, *Phys. Rev. Lett.* **76**, 664 (1996); L. Bellaiche, S.-H. Wei, and A. Zunger, *Phys. Rev. B* **54**, 17 568 (1996).
- <sup>22</sup>W. Shan, W. Walukiewicz, J. W. Ager III, E. E. Haller, J. F. Geisz, D. J. Friedman, J. M. Olson, and S. R. Kurtz, *Phys. Rev. Lett.* **82**, 1221 (1999).
- <sup>23</sup>J. D. Perkins, A. Mascarenhas, Y. Zhang, J. F. Geisz, D. J. Friedman, J. M. Olson, and S. R. Kurtz, *Phys. Rev. Lett.* **82**, 3312 (1999).
- <sup>24</sup>E. D. Jones, N. A. Modline, A. A. Allerman, S. R. Kurtz, A. F. Wright, S. T. Tozer, and X. Wei, *Phys. Rev. B* **60**, 4430 (1999).
- <sup>25</sup>T. Mattila, S.-H. Wei, and A. Zunger, *Phys. Rev. B* **60**, R11 245 (1999).
- <sup>26</sup>Y. Zhang, A. Mascarenhas, H. P. Xin, and C. W. Tu, *Phys. Rev. B* **61**, 4433 (2000).
- <sup>27</sup>Y. Zhang, A. Mascarenhas, H. P. Xin, and C. W. Tu, *Phys. Rev. B* **61**, 7479 (2000).
- <sup>28</sup>D. G. Thomas and J. J. Hopfield, *Phys. Rev.* **150**, 680 (1966).
- <sup>29</sup>X. Liu, S. G. Bishop, J. N. Baillargeon, and K. Y. Cheng, *Appl. Phys. Lett.* **63**, 208 (1993).
- <sup>30</sup>S. Miyoshi, H. Yaguchi, K. Onabe, R. Ito, and Y. Shiraki, *J. Cryst. Growth* **145**, 87 (1994).
- <sup>31</sup>H. Yaguchi, S. Miyoshi, G. Biwa, M. Kibune, K. Onabe, Y. Shiraki, and R. Ito, *J. Cryst. Growth* **170**, 353 (1997).
- <sup>32</sup>J. A. Van Vechten, *Phys. Rev.* **182**, 891 (1969).
- <sup>33</sup>H. Yaguchi, *J. Cryst. Growth* **189/190**, 500 (1998).
- <sup>34</sup>H. P. Xin, C. W. Tu, Y. Zhang, and A. Mascarenhas, *Appl. Phys. Lett.* **76**, 1267 (2000).
- <sup>35</sup>L. Bellaiche, S. H. Wei, and A. Zunger, *Phys. Rev. B* **56**, 10 233 (1997).
- <sup>36</sup>P. J. Wiesner, R. A. Street, and H. D. Wolf, *Phys. Rev. Lett.* **35**, 1366 (1975).
- <sup>37</sup>P. Migliorato, G. Margaritondo, P. Perfetti, and D. Margadonna, *Solid State Commun.* **14**, 893 (1974).
- <sup>38</sup>J. L. Merz, R. A. Faulker, and P. J. Dean, *Phys. Rev.* **188**, 1228 (1969).
- <sup>39</sup>D. Gershoni, E. Cohen, and A. Ron, *J. Lumin.* **34**, 83 (1985).
- <sup>40</sup>Y. Zhang, J. S. Zheng, D. L. Mi, B. Z. Yan, and B. X. Wu, *J. Phys.: Condens. Matter* **2**, 5219 (1990).
- <sup>41</sup>H. Mariette and J. Chevallier, *Solid State Commun.* **29**, 263 (1979).
- <sup>42</sup>J. H. Collet, J. A. Kash, D. J. Wolford, and J. Thompson, *J. Phys. C* **16**, 1283 (1983).
- <sup>43</sup>P. Leroux-Hugon and H. Mariette, *Phys. Rev. B* **30**, 1622 (1984).
- <sup>44</sup>H. Mariette, *Physica B* **146**, 286 (1987).

- <sup>45</sup>B. Gil and H. Mariette, *Phys. Rev. B* **35**, 7999 (1987).
- <sup>46</sup>D. J. Woford, B. G. Streetman, and J. Thompson, *J. Phys. Soc. Jpn.* **49**, 223 (1980).
- <sup>47</sup>Landolt-Bornstein, *Numerical Data and Functional Relationships in Science and Technology* (Springer-Verlag, New York, 1982), Group III, Vol. 17a.
- <sup>48</sup>E. C. Lightowers, J. C. North, and O. G. Lorimor, *J. Appl. Phys.* **45**, 2191 (1974).
- <sup>49</sup>H. Yaguchi, S. Miyoshi, H. Arimoto, S. Saito, H. Akiyama, K. Onabe, Y. Shiraki, and R. Ito, *Solid-State Electron.* **41**, 231 (1997).
- <sup>50</sup>C. J. Hwang, *Phys. Rev. B* **8**, 646 (1973).
- <sup>51</sup>P. J. Dean, *J. Lumin.* **1-2**, 398 (1970).
- <sup>52</sup>E. Cohen and M. D. Sturge, *Phys. Rev. B* **15**, 1039 (1977).
- <sup>53</sup>Y. Zhang, *Phys. Rev. B* **45**, 9025 (1992).